Journal of Engineering and Applied Sciences 12 (23): 7257-7264, 2017
ISSN: 1816-949X

Corrosion Fatigue Crack Propagation Behavior of Friction Stirred Dissimilar Metal Welds in 3.5% NaCl Solution by Chromate and Molybdate Inhibition

[1,2]F.X. Arif Wahyudianto, [1]Mochammad Noer Ilman, [1]Priyo Tri Iswanto and [1]Kusmono
[1]Department of Mechanical and Industrial Engineering, Gadjah Mada University, Yogakarta, Indonesia
[2]Department of Maritime, State Polytechnic of Samarinda, Samarinds, Indonesia

Abstract: The purpose of this investigation is to study the effects of molybdate and chromate inhibitors on the fatigue crack propagation behavior of friction stirred dissimilar metal welds between AA5083 and AA6061 in 3.5% NaCl solution. The chromate and molybdate inhibitors were added to 3.5% NaCl solution at various concentrations of 0.1, 0.3 and 0.5%. A corrosion test was conducted using electrochemical polarization technique to study the effectiveness of the inhibitors. Fatigue crack propagation test was conducted using a sinusoidal load with constant load amplitude and stress Ratio (R) of 0.1. To allow corrosion and fatigue to occur a low load frequency typically of 11 Hz was used. Results of this obsevation showed that the addition of chromate and molybdate inhibitors improved both resistance to corrosion and fatigue crack propagation performance, especially in the initial stages of propagation.

Key words: Molybdate, chromate inhibitor, dissimilar friction stir welding, corrosion fatigue, crack, propagation

INTRODUCTION

Aluminum alloys AA5083 and AA6061 are widely applied in ship building industries due to their good corrosion resistance, low weight and high strength (Ferraris and Volpone, 2005). Both alloys can be welded using conventional welding processes, i.e., MIG and TIG welding. However, welding of dissimilar aluminum alloys using these welding processes are difficult since they have different properties such as AA5083 is non-heat treatable while AA6061 is heat treatable. Recently, Friction Stir Welding (FSW) which is a welding in solid-state process has become a preferred welding method for joining aluminum alloys, either similar or dissimilar (Mishra and Ma, 2005). Some research a dissimilar welding of AA5083 and AA6061 have been conducted with specific attentions are paid to factors such as welding conditions and combination of materials that are welded (Gan *et al*., 2008; Ghaffarpour *et al*., 2013; Shigematsu *et al*., 2003). It has been known that the welds mechanical properties are influenced by a combination of the type of joint (similar or dissimilar) and material.

The dissimilar friction weld joints between 5xxx and 6xxx series by welding FSW process have different mechanical properties and microstructure from the parent metal (Ghaffarpour *et al*., 2013; Aval *et al*., 2012; Sadeesh *et al*., 2014; Shigematsu *et al*., 2003) while recent studies have investigated fatigue crack growth properties of 6xxx and 5xxx alloy FSW welded (D'Urso *et al*., 2014; Hrishikesh *et al*., 2014; Gungor *et al*., 2014; Infante *et al*., 2016; Moreira *et al*., 2008; Zhou *et al*., 2005). In Engineering practice, AA5083 and AA6061 used for the ship building structure are exposed to the aggressive environment during service and at the same time, they are suffered from dynamic loads. This condition can cause failure known as corrosion fatigue, especially, at weld joints because the nugget zone of FSW welds has a lower strength than the parent material due to recrystallization.

The weld zones of FSW is an area that is sensitive to corrosion (Mishra and Ma, 2005). Aluminum alloy AA5xxx has better corrosion resistance than AA4xxx and AA6xxx series which are more susceptible to pitting corrosion (Hariri *et al*., 2013). Results of corrosion resistance and corrosion fatigue strength for aluminum alloys welded using FSW methods in NaCl solution has been reported previously (Abdulstaar *et al*., 2014; Chemin *et al*., 2015; Davoodi *et al*., 2016; Donatus *et al*., 2015; Fahimpour *et al*., 2012; Maggiolino and Schmid, 2008; Wang, 2008). The fatigue crack growth rates of aluminum alloy FSW welded in 3.5% NaCl are higher than in the air.

Corresponding Author: Mochammad Noer Ilman, Department of Mechanical and Industrial Engineering, Gadjah Mada University, Yogakarta, Indonesia

The aggressiveness of the corrosive environment (seawater) on the aluminum alloys can be controlled by using inhibitors such as chromate and molybdate. Recent studies have shown that chromate and molybdate in combination with other compounds provide an inhibition effect on corrosion, hence increasing the corrosion protection for aluminum alloy (Dorman and Lee, 2011; Ilman, 2014; Liu *et al*., 2002; Silva *et al*., 2005; Srinivasan *et al*., 2007). However, just little information exists about the effect of chromate and molybdate on corrosion and fatigue performance of friction stirred dissimilar metal weld between AA5083 and AA6061-T6. Therefore, the primary purpose of this research is to evaluate the mechanism of the addition of chromate and molybdate into a solution of 3.5% NaCl for controlling the corrosion fatigue crack propagation of friction stirred dissimilar metal welds between AA5083 and AA6061.

MATERIALS AND METHODS

Aluminum alloy AA5083 and AA6061-T6 plates with 3.0 mm thickness were used in this study. The chemical composition of the materials is given in Table 1. Friction Stir Welding (FSW) was performed with the tool rotating speed of 2280 rpm, tool traveling speed of 30 mm/min and tilt angle of 3°. The AA6061-T6 was located on the advancing side while AA 5083 on the retreating side (Fig. 1).

Microstructural observations were performed using an optical microscopy to study various zones in FSW joints including parent metal/Base Metal (BM) Heat Affected Zone (HAZ) thermomechanically affected zone (TMAZ) and Nugget Zone (NZ). The specimens were prepared using etchant of Keller reagent made of 5 mL HNO_3, 2 mL HF, 3 mL HCl and 190 mL of H_2O. Corrosion rates were measured using resiatance polarization technique with a reference electrode of Saturated Calomel (Hg_2Cl_2) Electrode (SCE) and the auxiliary electrode of Platinum (Pt). The corrosion rate measurements were taken from the weld regions in 3.5% NaCl solution with and without inhibitors (chromate and molybdate). The various of inhibitors concentration were 0.1, 0.3 and 0.5%.

The corrosion fatigue test was done using a servo-hydraulic testing machine with a load ratio (R) = 0.1, a frequency of 11 Hz and stress level used was 20% of yield stress. Specimens were prepared according to ASTM E647 standard. The specimens were immersed in an acrylic chamber containing various solutions. During fatigue test, crack lengths were measured using a traveling microscope. Subsequently, fracture surface in stable crack regions was observed and analyzed by a Scanning Electron Microscopy (SEM).

Table 1: Chemical composition of specimens (wt. %)

Aluminum alloy	Mg	Mn	Cu	Cr	Si	Fe	Al
AA5083	4.30	0.50	0.04	0.06	0.11	0.30	Bal
AA6061-T6	1.10	0.02	0.28	0.22	0.64	0.33	Bal

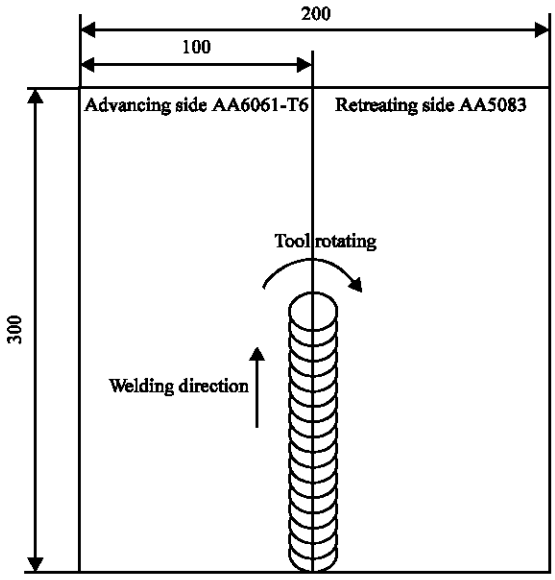

Fig. 1: The schematic illustration of friction stir welding process

RESULTS AND DISCUSSION

Microstructure: Figure 2 shows results of microstructural examination at cross section welds joints which are divided into Base Metal (BM), Heat Affected Zone (HAZ), Thermo Mechanically Affected Zone (TMAZ) and Nugget Zone (NZ). It can be seen that each zone has a different microstructure NZ has some variation in microstructure due to incomplete mixing during stirring. These microstructural variations cause differences in the corrosion resistance of the weld joints.

Base metal microstructures of both (AA6061 and AA5083-T6) reveal elongated grain structures with the grain orientation parallel to the direction of rolling (Fig. 2a and d). It can be seen that the grains microstructure of the AA6061-T6 is larger and more elongated than the grains in AA5083. Regions HAZ, TMAZ and NZ have different morphology and grain size compared to the base metal. In HAZ regions (Fig. 2e and h) 2 larger grains are resulted from grain growth under the influence heat. The shape and size of the grains in the region TMAZ are caused by combined effect of heat due to friction tool and mechanical stirring (Fig. 2b and g). Figure 3 shows that the mixing of the NZ during friction stirred welding process cannot be accomplished completely resulting in heterogeneity in

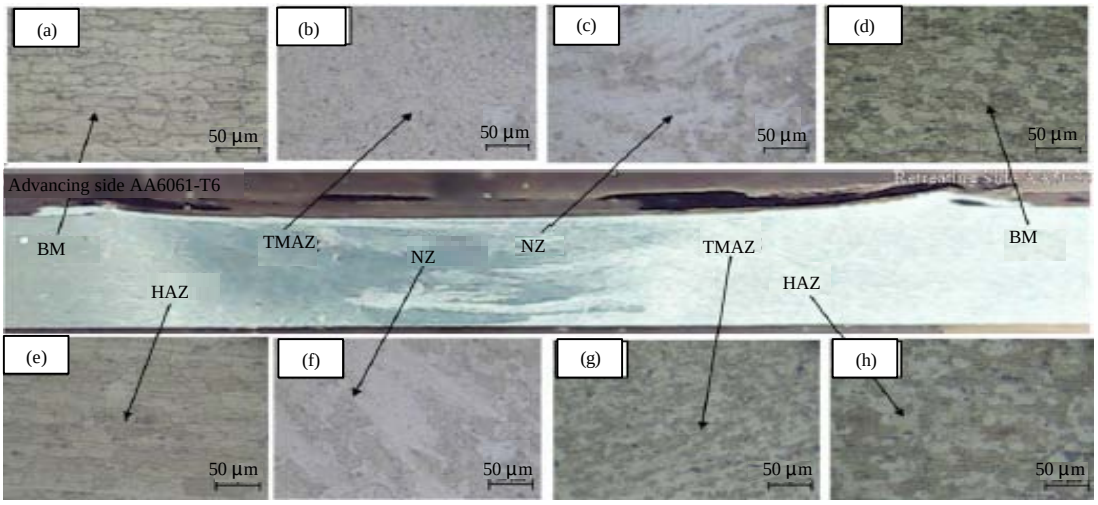

Fig. 2: A-H) Microstructure of BM, HAZ, TMAZ and NZ regions

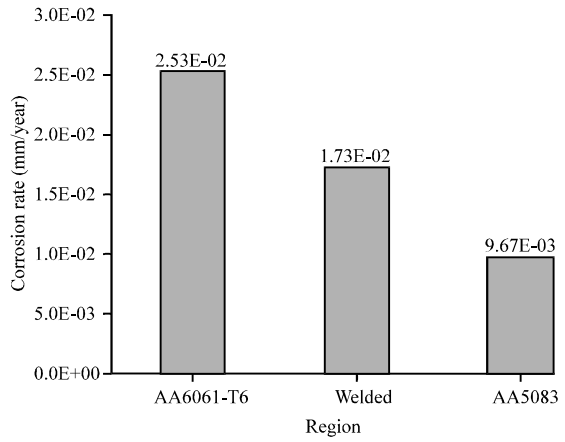

Fig. 3: Corrosion rate of base material and FSW welded

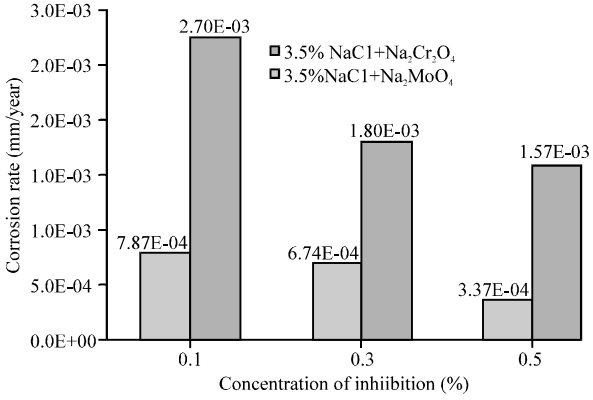

Fig. 4: Corrosion rate of FSW welded with various of inhibitor

weld nugget region. The NZ grain structure appears to be finer which is much smaller than the base metal as a result of recrystallization during stirring process (Ilman, 2014).

Corrosion behavior: Figure 3 shows corrosion rates of base materials (AA6061-T6 and AA5083) and FSW weld. It can be seen that the corrosion rate of AA6061 base metal is the highest while the lowest value of corrosion rate occurs in AA5083 base metal. The corrosion rate of the weld region falls between the two base materials. Figure 4 shows the values of corrosion rate of FSW welded with various inhibitors. It can be seen that the addition of both inhibitors lowers the rate of corrosion in joint FSW welds but the chromate inhibitor has the better resistance to corrosion rate than that of molybdate inhibitor. The effectiveness of the inhibitor can be seen from the Inhibition Efficiency (IE) which can be determined using the following Eq. 1:

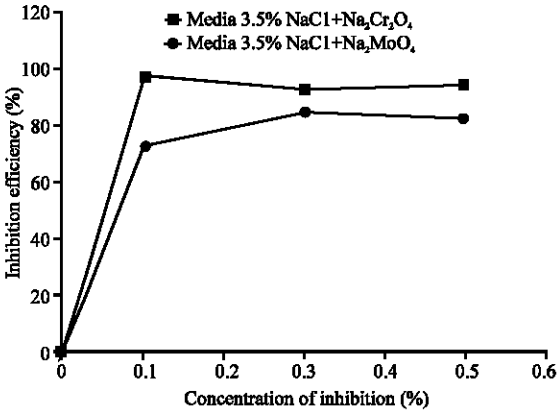

Fig. 5: Inhibitor efficiency

$$IE(\%) = \frac{i_0 - i}{i_0} \times (100\%) \quad (1)$$

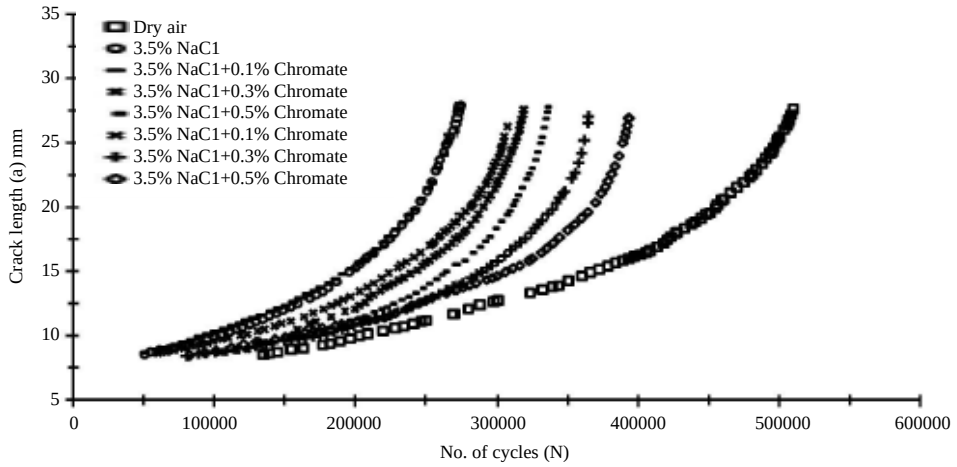

Fig. 6: Fatigue life of FSW welded in dry air and 3.5% NaCl solution with various levels of chromates and molybdates

where, i and i_o are corrosion rate with and without inhibitor, respectively. Figure 5 shows the efficiency of inhibitor as a function of concentration of inhibitor. It can be seen that the addition of 0.1% both chromate and molybdate inhibitor cause a sharp increase in efficiency. Further addition of the inhibitor concentration achieves constant values with no more significant increase with inhibitor addition. Containing inhibitor of chromate in the conversion coating form or as coating pigments inhibit the Al substrate anodic dissolution in an acidic environment by forming Chromium (Cr) and Aluminum (Al) oxides combination. Once the surface was covered by chromium oxide, then the contact between Al and corrosive solution is isolated. So that the specimen's surface becomes protected from dissolution effectively (Kloet *et al*., 2004). Result of this research show that the use of chromate as inhibitors in 3.5% NaCl solution is an extremely effective to reduce the rate of corrosion of the aluminum surface (Grilli *et al*., 2011; Silva *et al*., 2005; Gupta *et al*., 2014).

Corrosion fatigue crack propagation rates: Corrosion fatigue tests results of the FSW joints specimen in dry air and 3.5% NaCl solution with various inhibitors contents are represented by plotting crack length (a) vs. number of cycles (N) as presented in Fig. 6. It is seen that corrosive environment causes a decrease in FSW joint fatigue life than the friction stired welds fatigue crack growth in the air and the addition of inhibitor in 3.5% NaCl solution can reduced. The most effective of inhibitors in increasing resistance of fatigue crack growth is observed as its fatigue life. The fatigue life of the weld in the atmosphere is around 510,000 cycles whereas in media 3.5% NaCl the fatigue life is reduced to approximately 270,000 cycles.

Table 2: Paris constants

Environment	C	n
Dry air	5.83E-10	2.44
3.5% NaCl	6.23E-10	2.69
3.5% NaCl+0.1% Chromate	4.56E-10	2.88
3.5% NaCl+0.3% Chromate	7.22E-10	2.62
3.5% NaCl+0.5% Chromate	2.45E-10	3.19
3.5% NaCl+0.1% Molybdate	3.30E-10	2.99
3.5% NaCl+0.3% Molybdate	1.14E-10	3.56
3.5% NaCl+0.5% Molybdate	1.39E-10	3.38

Chromate concentration of 0.1% in the solution does not significantly affect the fatigue resistance of the material but the significant increase is observed if the chromate concentrations are increased up to 0.3 and 0.5%, Another inhibitor named molybdate, at a concentration of 0.1% already provides corrosion inhibition. At 0.5% molybdate, the ability to inhibit corrosion fatigue crack propagation rates in 3.5% NaCl increasing.

The fatigue crack propagation rates of FSW welds in the air and 3.5% NaCl solution with various chromate and molybdate can be studied by plotting da/dN versus ΔK as shown in Fig. 7 and 8. The fatigue crack growth curves are divided into three parts (Stage 1-3). The stage 1 represents crack initiation whereas stable fatigue crack propagation occurs in study 2 which is based on the Paris low as given by the $da/dN = C(\Delta K)^n$ where C and n are Paris constant where its value is da/dN at $\Delta K = 1$ MPa$\sqrt{m}$ and n are the slopes of the line. The results are shown in Table 2. It can be seen that the value of C and n of the weld fatigued in the air is lower than that tested in 3.5% NaCl. Referring to Fig. 9, 10 and Table 2, it is seen that the fatigue specimen in air condition produced lower crack growth rate than in the corrosive environment. In the 3.5% NaCl solution, crack growth rate of the weld increases at low ΔKvalue, typically below 11 MPa$\sqrt{m}$. The additions of inhibitors inhibit the growth rate of fatigue

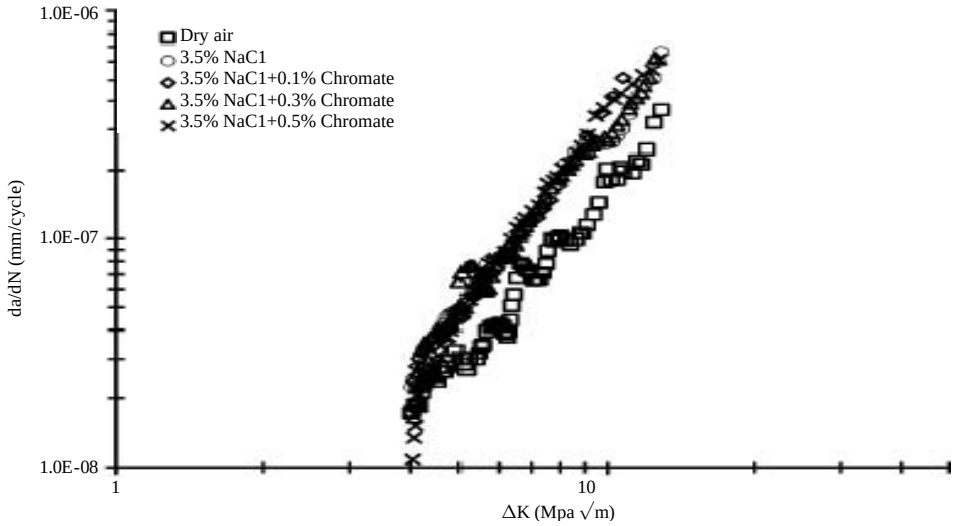

Fig. 7: Fatigue crack propagation rate of FSW welded with various levels of chromates

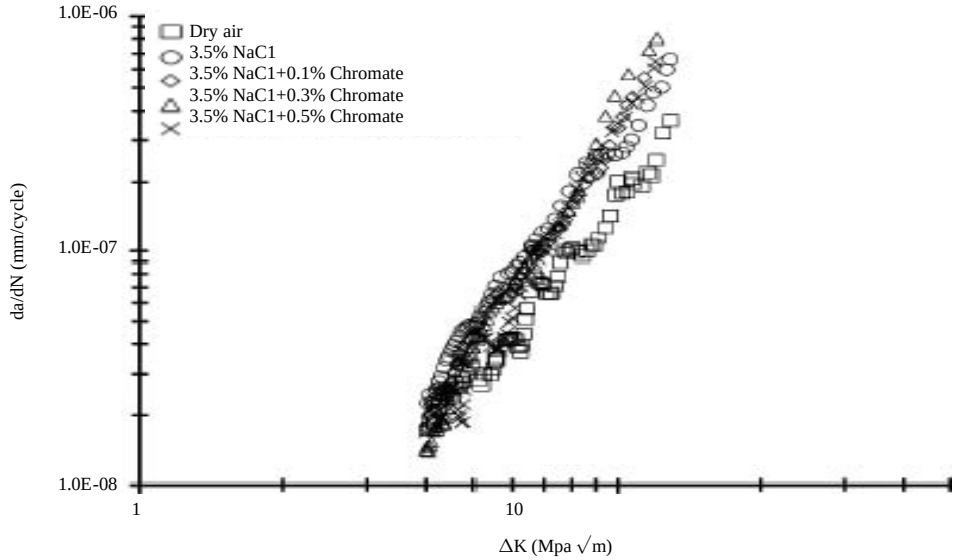

Fig. 8: Fatigue crack propagation rate of FSW welded with various levels of molybdates

crack propagation rate, especially in the early stages. Additions of inhibitors in this investigation reduced C but increased n values of Paris constants hence lowering da/dN at low ΔK.

The addition of molybdate into a solution of NaCl in the study has a better ability to resist fatigue crack propagation rate than the chromate (Fig. 6). Molybdate completely inhibits the rate of fatigue crack propagation at high load and low frequency, quantified by the reduced crack growth rate to that typical of ultra-high vacuum, reduction in surface crack facets typical of hydrogen embrittlement and crack arrest. Chromate did not produce such complete inhibition (Warner *et al*., 2009).

Fractured surface after fatigue test in air, solution of 3.5, 3.5 NaCl+0.5% chromate and 3.5 NaCl+0.5% molybdate can be seen in Fig. 11. It is seen that the surface fractured of the weld in air (Fig. 11a) is uniform from the beginning to the end of the crack suggesting that fatigue area is relatively large. At the initiation of crack propagation for weld specimen in 3.5% NaCl media (Fig. 11b), there are many of corrosion, pits due to local acidification which occurs at the crack tip (Warner and Gangloff, 2012) while in the dry air is not found traces of corrosion. At this stage of the propagation medium, cleavage morphology was found and some of the corrosion deposits appear on the fracture surface. In the

late stages of propagation because the crack growth rate is high, there are no corrosion deposits appear on the surface of the fracture ands there are lots of little cleavage face.

The addition of chromate (0.3 and 0.5%) or molybdate to 3.5% NaCl solution is proved to be effective in inhibiting the corrosion fatigue crack propagation rates of FSW welds different types but the addition of inhibitor in the solution does not give effect to the rate of crack propagation at the end of fracture. Chromate and molybdate on fatigue crack growth process also serve to stabilize the passive layer of the crack tip that reduces the production of Hydrogen (H) (Ilman, 2014; Warner *et al*., 2009; Warner and Gangloff, 2012).

Molybdate in 3.5% NaCl solution is also able to reduce acidification cracked by hydrolysis. The corrosion fatigue crack propagation rates on FSW weld joint between the different types of AA5083 and AA6061-T6 by adding molybdate in 3.5% NaCl solution can give better the rate of fatigue crack propa gation retardation than chromate. Corrosion fatigue crack propagation of fractured in 3.5% NaCl solution, 3.5 NaCl + 0.5% chromate solution and 3.5% NaCl solution+0.5% molybdate propagated by transgranular in all test conditions. SEM image showing the specimen fracture surface in a different environment after the corrosion fatigue crack propagation test shown in Fig. 12. This condition clearly shows a mixture of quasi-cleavage and ductile striations on fracture surfaces for all specimens. Figure 12a shown that the cracks are marked by the presence of striations typical of fatigue and Fig. 12b and c and are appear intergranular crack with secondary crack.

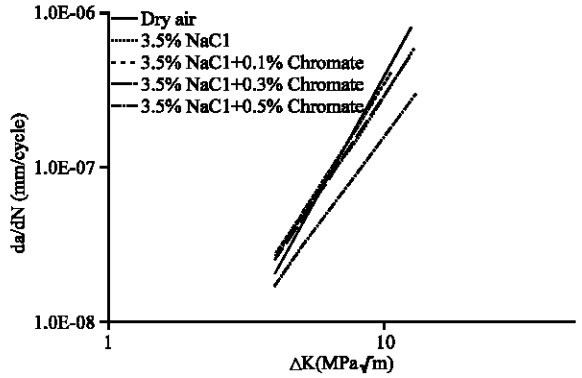

Fig. 9: Trendlines taken from region 2 of FSW welded with various levels of chromates

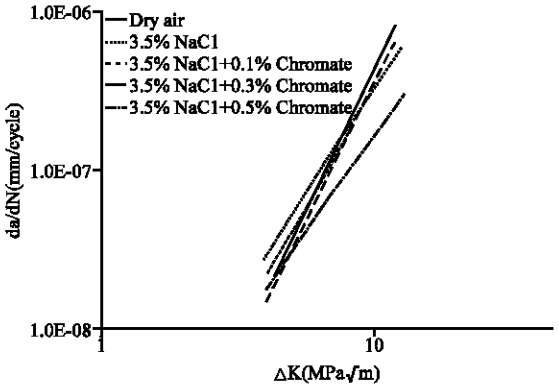

Fig. 10: Trendlines taken from region 2 of FSW welded with various levels of molybdates

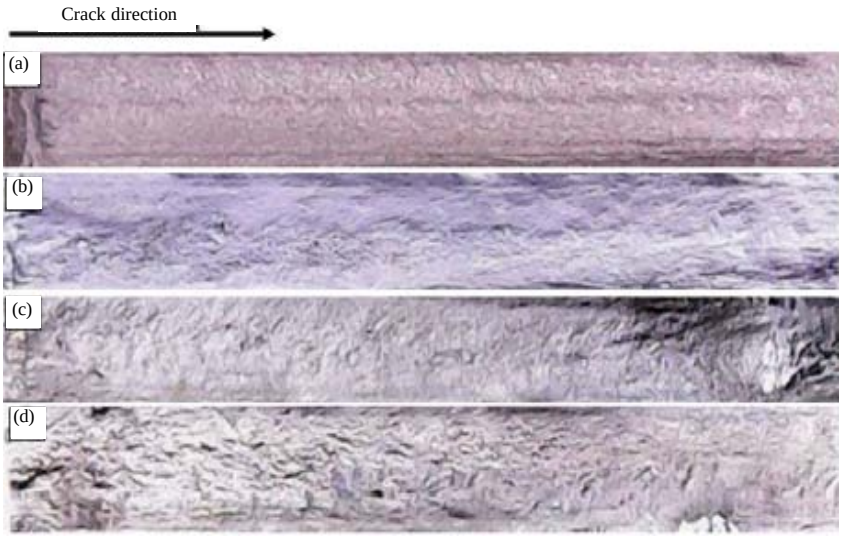

Fig. 11: Macro photographs of fractured surfaces of welded specimen tested in: a) Air ; b) 3.5% NaCl; c) 3.5% NaCl+ 0.5% $Na_2Cr_2O_4$ and d) 3. 3.5% NaCl+0.5% Na_2MoO_4

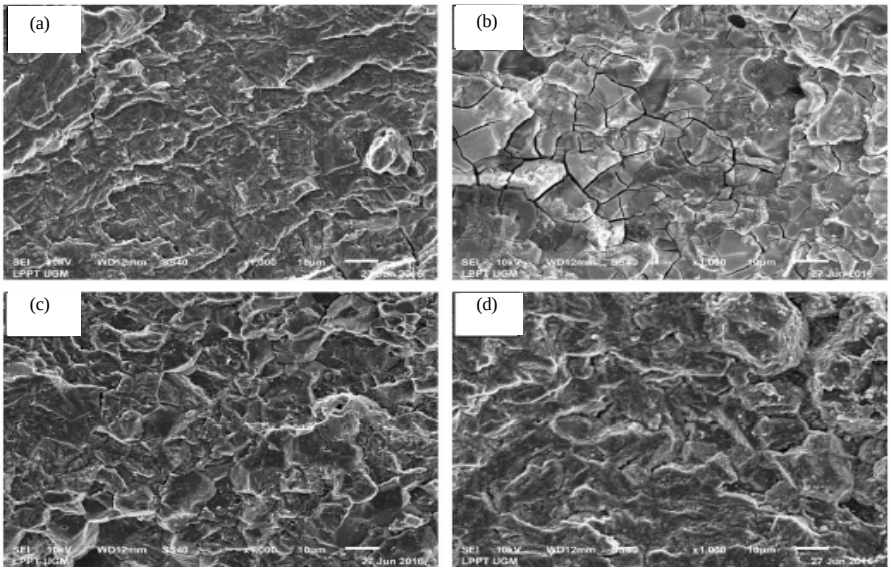

Fig. 12: SEM photographs of ractured surfaces of welded specimen tested in: a) Air; b) 3.5% NaCl; c) 3.5% NaCl+0.5% $Na_2Cr_2O_4$ and d) 3.5% NaCl+0.5% Na_2MoO_4

CONCLUSION

The effect of adding chromate and molybdate in this study can be concluded as follows. The addition of chromate and molybdate able to reduce the corrosion rate of the dissimilar FSW joints between AA5083 and AA6061-T6 but with an increased concentration of the inhibitor is not always accompanied by a decrease in corrosion rate. This happens due to the lack of structure in the area homogenous NZ formed during welding. The test results showed that polarization resistant chromate could withstand corrosion rate of dissimilar FSW joints between AA5083 and AA6061-T6 is more effective than the molybdate while in corrosion fatigue crack propagation test showed molybdate better at curbing fatigue crack propagation.

ACKNOWLEDGEMENT

This research was funded by the doctoral grant of Ministry of Research, Technology and Higher Education Republic of Indonesia.

REFERENCES

Abdulstaar, M., M. Mhaede, M. Wollmann and L. Wagner, 2014. Investigating the effects of bulk and surface severe plastic deformation on the fatigue, corrosion behaviour and corrosion fatigue of AA5083. Surf. Coat. Technol., 254: 244-251.

Aval, H.J., S. Serajzadeh, N.A. Sakharova, A.H. Kokabi and A. Loureiro, 2012. A study on microstructures and residual stress distributions in dissimilar friction-stir welding of AA5086-AA6061. J. Mater. Sci., 47: 5428-5437.

Chemin, A., D. Spinelli, W.B. Filho and C. Ruchert, 2015. Corrosion fatigue crack growth of 7475 T7351 Aluminum alloy under flight simulation loading. Procedia Eng., 101: 85-92.

Davoodi, A., Z. Esfahani and M. Sarvghad, 2016. Microstructure and corrosion characterization of the interfacial region in dissimilar friction stir welded AA5083 to AA7023. Corros. Sci., 107: 133-144.

Donatus, U., G.E. Thompson, X. Zhou, J. Wang and A. Cassell *et al*., 2015. Corrosion susceptibility of dissimilar friction stir welds of AA5083 and AA6082 alloys. Mater. Charact., 107: 85-97.

Dorman, S.E.G. and Y. Lee, 2011. Effect of chromate primer on corrosion fatigue in Aluminum alloy 7075. Procedia Eng., 10: 1220-1225.

D'Urso, G., C. Giardini, S. Lorenzi and T. Pastore, 2014. Fatigue crack growth in the welding nugget of FSW joints of a 6060 Aluminum alloy. J. Mater. Process. Technol., 214: 2075-2084.

Fahimpour, V., S.K. Sadrnezhaad and F. Karimzadeh, 2012. Corrosion behavior of Aluminum 6061 alloy joined by friction stir welding and gas tungsten arc welding methods. Mater. Des., 39: 329-333.

Ferraris, S. and L.M. Volpone, 2005. Aluminum alloys in third millennium shipbuilding: Materials, technologies, perspectives. Proceedings of the 5th International Conference on Forum on Aluminium Ships, October 11-13, 2005 insTECH Publisher, Tokyo, Japan, pp: 1-11.

Gan, W., K. Okamoto, S. Hirano, K. Chung and C. Kim *et al*., 2008. Properties of friction-stir welded Aluminum alloys 6111 and 5083. J. Eng. Mater. Technol., 130: 031007-031021.

Ghaffarpour, M., S. Kolahgar, B.M. Dariani and K. Dehghani, 2013. Evaluation of dissimilar welds of 5083-H12 and 6061-T6 produced by friction stir welding. Metall. Mater. Trans. A., 44: 3697-3707.

Grilli, R., M.A. Baker, J.E. Castle, B. Dunn and J.F. Watts, 2011. Corrosion behaviour of a 2219 Aluminum alloy treated with a chromate conversion coating exposed to a 3.5% NaCl solution. Corros. Sci., 53: 1214-1223.

Gungor, B., E. Kaluc, E. Taban and A. Sik, 2014. Mechanical, fatigue and microstructural properties of friction stir welded 5083-H111 and 6082-T651 Aluminum alloys. Mater. Des., 56: 84-90.

Gupta, R.K., B.R.W. Hinton and N. Birbilis, 2014. The effect of chromate on the pitting susceptibility of AA7075-T651 studied using potentiostatic transients. Corros. Sci., 82: 197-207.

Hariri, M.B., S.G. Shiri, Y. Yaghoubinezhad and M.M. Rahvard, 2013. The optimum combination of tool rotation rate and traveling speed for obtaining the preferable corrosion behavior and mechanical properties of friction stir welded AA5052 Aluminum alloy. Mater. Des., 50: 620-634.

Hrishikesh, D.A.S., D. Chakraborty and T.K. PAL, 2014. High-cycle fatigue behavior of friction stir butt welded 6061 Aluminum alloy. Trans. Nonferrous Met. Soc. China, 24: 648-656.

Ilman, M.N., 2014. Chromate inhibition of environmentally assisted fatigue crack propagation of Aluminum alloy AA 2024-T3 in 3.5% NaCl solution. Intl. J. Fatigue, 62: 228-235.

Infante, V., D.F.O. Braga, F. Duarte, P.M.G. Moreira and M.D. Freitas *et al*., 2016. Study of the fatigue behaviour of dissimilar Aluminum joints produced by friction stir welding. Intl. J. Fatigue, 82: 310-316.

Kloet, J.V., W. Schmidt, A.W. Hassel and M. Stratmann, 2004. The role of chromate in filiform corrosion inhibition. Electrochim. Acta, 49: 1675-1685.

Liu, X.F., S.J. Huang and H.C. Gu, 2002. Crack growth behaviour of high strength Aluminum alloy in 3.5% NaCl solution with corrosion inhibiting pigments. Intl. J. Fatigue, 24: 803-809.

Maggiolino, S. and C. Schmid, 2008. Corrosion resistance in FSW and in MIG welding techniques of AA6XXX. J. Mater. Process. Technol., 197: 237-240.

Mishra, R.S. and Z.Y. Ma, 2005. Friction stir welding and processing. Mater. Sci. Eng.: R: Rep., 50: 1-78.

Moreira, P.M.G.P., A.M.P.D. Jesus, A.S. Ribeiro and P.M.S.T.D. Castro, 2008. Fatigue crack growth in friction stir welds of 6082-T6 and 6061-T6 Aluminum alloys: A comparison. Theor. Appl. Fract. Mech., 50: 81-91.

Sadeesh, P., M.V. Kannan, V. Rajkumar, P. Avinash and N. Arivazhagan *et al*., 2014. Studies on friction stir welding of AA 2024 and AA 6061 dissimilar metals. Procedia Eng., 75: 145-149.

Shigematsu, I., Y.J. Kwon, K. Suzuki, T. Imai and N. Saito, 2003. Joining of 5083 and 6061 Aluminum alloys by friction stir welding. J. Mater. Sci. Lett., 22: 353-356.

Silva, J.W.J., E.N. Codaro, R.Z. Nakazato and L.R.O. Hein, 2005. Influence of chromate, Molybdate and Tungstate on pit formation in Chloride medium. Appl. Surf. Sci., 252: 1117-1122.

Srinivasan, P.B., W. Dietzel, R. Zettler, J.F.D. Santos and V. Sivan, 2007. Effects of inhibitors on corrosion behaviour of dissimilar Aluminum alloy friction stir weldment. Corros. Eng. Sci. Technol., 42: 161-167.

Wang, R., 2008. A fracture model of corrosion fatigue crack propagation of Aluminum alloys based on the material elements fracture ahead of a crack tip. Intl. J. Fatigue, 30: 1376-1386.

Warner, J.S. and R.P. Gangloff, 2012. Molybdate inhibition of corrosion fatigue crack propagation in precipitation hardened Al-Cu-Li. Corros. Sci., 62: 11-21.

Warner, J.S., S. Kim and R.P. Gangloff, 2009. Molybdate inhibition of environmental fatigue crack propagation in Al-Zn-Mg-Cu. Intl. J. Fatigue, 31: 1952-1965.

Zhou, C., X. Yang and G. Luan, 2005. Fatigue properties of friction stir welds in Al 5083 alloy. Scr. Mater., 53: 1187-1191.